Proceedings of the ASME 2020 International Technical Conference and Exhibition on Packaging and Integration of Electronic and Photonic Microsystems
InterPACK2020
October 27 - 29, 2020, Anaheim, California, USA

InterPACK2020-2542

ULTRA-COMPACT MICRO-SCALE HEAT EXCHANGER FOR ADVANCED THERMAL MANAGEMENT IN DATACENTERS

Raffaele L. Amalfi
Todd Salamon

Efficient Energy Transfer Department
Nokia Bell Laboratories
Murray Hill, New Jersey, USA
Email: raffaele.amalfi@nokia-bell-labs.com

Filippo Cataldo

Micro-Cooling Laboratory
Provides Metalmeccanica S.r.l.
Latina, Italy
Email: f.cataldo@provides.it

Jackson B. Marcinichen[1]
John R. Thome[1,2]

[1]JJ Cooling Innovation Sàrl
[2]Ecole Polytechnique Fédérale de Lausanne
Lausanne, Switzerland
Email: john.thome@jjcooling.com

ABSTRACT

The present study is focused on the experimental characterization of two-phase heat transfer performance and pressure drops within an ultra-compact heat exchanger (UCHE) suitable for electronics cooling applications. In this specific work, the UCHE prototype is anticipated to be a critical component for realizing a new passive two-phase cooling technology for high-power server racks, as it is more compact and lighter weight than conventional heat exchangers. This technology makes use of a novel combination of thermosyphon loops, at the server-level and rack-level, to passively cool an entire rack. In the proposed two-phase cooling technology, a smaller form factor UCHE is used to transfer heat from the server-level thermosyphon cooling loop to the rack-level thermosyphon cooling loop, while a larger form factor UCHE is used to reject the total heat from the server rack into the facility-level cooling loop. The UCHE is composed of a double-side-copper finned plate enclosed in a stainless steel enclosure. The geometry of the fins and channels on both sides are optimized to enhance the heat transfer performance and flow stability, while minimizing the pressure drops. These features make the UCHE the ideal component for thermosyphon cooling systems, where low pressure drops are required to achieve high passive flow circulation rates and thus achieve high critical heat flux values. The UCHE's thermal-hydraulic performance is first evaluated in a pump-driven system at the Laboratory of Heat and Mass Transfer (LTCM-EPFL), where experiments include many configurations and operating conditions. Then, the UCHE is installed and tested as the condenser of a thermosyphon loop that rejects heat to a pumped refrigerant system at Nokia Bell Labs, in which both sides operate with refrigerants in phase change (condensation-to-boiling). Experimental results demonstrate high thermal performance with a maximum heat dissipation density of 5455 ($kW/m^3/K$), which is significantly larger than conventional air-cooled heat exchangers and liquid-cooled small pressing depth brazed plate heat exchangers. Finally, a thermal performance analysis is presented that provides guidelines in terms of heat density dissipations at the server- and rack-level when using passive two-phase cooling.

NOMENCLATURE

Roman

D	depth, (m)
f	enhancement factor, (–)
H	height, (m)
N	number of servers, (–)
P	pressure, (Pa)
Q	heat load or power, (W)
R	thermal resistance, (K/W)
T	temperature, (K)
W	width, (m)

Greek

Δ	difference, (–)

Subscripts

CPU	CPU

rack	rack
server(s)	server(s)
th	thermal
therm	thermosyphon
TIM	TIM
tot	total
water	water

Acronyms

CDU	Cooling Distribution Unit
CPU	Central Processing Unit
CRAC	Computer Room Air Conditioner
FR	Filling ratio
ICT	Information and Communications Technology
IT	Information Technology
LMTD	Logarithmic Mean Temperature Difference
PHE	Plate Heat Exchanger
TCO	Total costs of Ownership
TIM	Thermal Interface Material
UCHE	Ultra-Compact Heat Exchanger

INTRODUCTION

In 2018 datacenter energy consumption was about 90 TWh in the US (corresponding to 3% of the total energy consumption) [1]; In 2019 European datacenters have consumed about 259 TWh (corresponding to 1.7% of the world's total energy consumption) [2, 3]. Approximately, between 25% and 55% of this energy is required by conventional air-cooling systems deployed today. They require fans, blowers and CRACs for the recirculation of cold air in the datacenter space to keep the temperature of the CPUs, and other IT hardware components, within their maximum allowable values for proper operation [4]. Datacenter energy consumption is expected to grow in the near future, if particular attention is not given to cooling, which can be a significant portion of the overall datacenter energy consumption (this also depends on the size, location and server usage). Edge datacenters also represent a fast-growing market that is needed to handle system requirements for emerging smart cities, manufacturing, autonomous vehicles, augmented reality, and many others. The demand by servers storing digital data from billions of smartphones, tablets and internet-connected devices grows exponentially. It has been predicted that by 2025 the ICT sector will use 20% of world's electricity and emit up to 5,5% of all CO_2 emissions [5]. Moreover, billions of internet-connected devices could produce up to 14% of global CO_2 by 2040 [6]. It is clear that current datacenters are not green, challenging to manage and expensive to run and this can be justified by the inefficient cooling systems deployed today [7]. Major players in this space are investigating more advanced thermal management solutions for their datacenters and an overview of ongoing research activities and technologies can be found in Amalfi et al. [8]. Based on the contents mentioned in this section, it is extremely important to develop novel cooling technologies that strongly reduce electricity consumption and CO_2 emissions.

NOVEL TWO-PHASE COOLING TECHNOLOGY

Figure 1 presents the envisioned cooling technology pursued in this study which operates with numerous mini-scale thermosyphons in parallel in order to dissipate the heat generated by the large heat sources of the individual servers. Then, the heat is transferred to macro-scale thermosyphons, equipped with an overhead compact heat exchanger that rejects the total heat from the server rack into the datacenter water cooling loop. This technology can also target heat reuse applications as the high temperature of the water cooling loop can become a very profitable free source of thermal energy to sell to a district heating network or to preheat boiler feed water in a power plant (as examples).

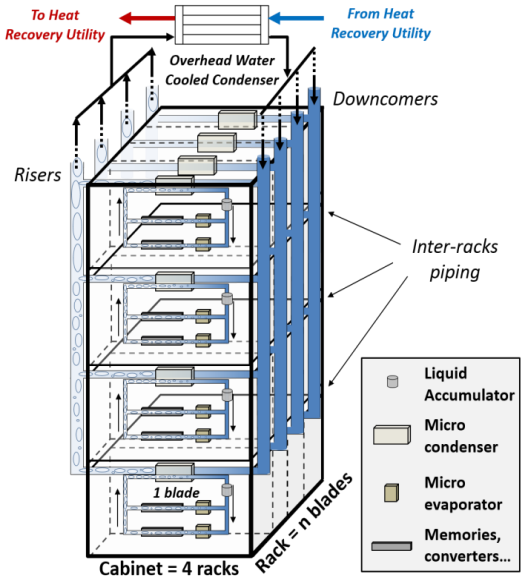

Figure 1 – Advanced two-phase cooling technology applied to a server rack, as reported in Amalfi et al. [9]. Passive two-phase can be implemented to cool individual CPUs or multiple heat sources at the server-level. This technology can also achieve significant energy capture from the IT equipment. Note that the UCHE design can be used in place of micro-condensers and overhead water cooled condenser.

The main advantages of the proposed two-phase cooling technology compared to existing approaches are the following:

- Implement passive two-phase heat removal from server-to-rack-level that does not require active control and allows a significant reduction in fan power requirements at rack- and facility-level;
- Ensure scalability toward high heat density dissipations thanks to the nature of two-phase flow that uses the latent heat of the boiling process instead of the sensible

heat associated to the temperature rise of the coolant in existing air- and liquid-cooling technologies.

- Expected rack heat density dissipations are in the order of 50-100 kW (or higher), therefore this technology will be able to handle power requirements of next-generation telecommunications and high-performance computing datacenters.
- Remove CDU for recirculating the coolant at rack-level which is beneficial to reduce complexity and costs;
- Provide high heat transfer effectiveness on the heat rejection side and low overall thermal resistance due to the use of passive two-phase cooling along with the optimized overhead condenser;
- Offer holistic modular design strategy allowing flexible deployment to address standard and non-standard (e.g. heat re-use) applications. In addition, can be used to retrofit existing datacenters or specifically designed for new datacenters;
- Minimize TCO due to the reduction in energy costs, site infrastructure costs (i.e. compact and less expensive cooling system at the facility-level, less building floor space) and operating expenses (i.e. less maintenance and failure risks).
- Represent a green cooling technology because of the use of low GWP refrigerants (less than 1), which are non-toxic and non-flammable. Also, refrigerants are dielectric fluids, therefore do not damage the electronics and are in vapor phase at the ambient condition.

As can be observed from Figure 1, the micro-condensers (server-to-rack connections) and the overhead water cooled condenser at the rack-level represent the critical components due to their form factor and heat load requirements. This study proposes the UCHE as a suitable candidate to fulfill those metrics, then experimentally assess UCHE's two-phase heat transfer performance and finally, presents a scaling analysis to find the best trade-off between form factor and performance.

TEST FACILITIES

This section provides an overview of the two test facilities built at LTCM-EPFL and Nokia Bell Labs respectively. The schematic of the LTCM's test facility is reported in Figure 2, where the goal is the characterization of the two-phase heat transfer performance of a water-cooled UCHE operating in pump mode (active two-phase loop) using R236fa and R134a as the working fluids.

The subcooled refrigerant is circulated within the loop using a gear pump that is magnetically coupled to a variable speed motor to set the desired mass flow rate. The latter is measured by a Coriolis flow meter located upstream of the first electrical preheater that is used to preheat the refrigerant. A second electrical preheater is incorporated in the loop to further adjust the subcooling or to preboil the refrigerant before entering the test section (UCHE). Needle valves are installed at the inlet of each preheater to minimize back flow and two-phase flow instabilities. The heat load inside the UCHE is transferred from the primary (refrigerant) side to the secondary (water) side in case of condensing flow, and in the other direction for evaporating flow. The test section is fully equipped with K-type thermocouples and pressure transducers to measure fluid temperatures, absolute pressures and total pressure drops across each component of the test facility. A double by-pass loop is built upstream of the test section to control the flow direction of the two fluids within the UCHE. In particular, downward refrigerant flow is used for condensation tests (gravity-assisted flow), while upward refrigerant flow (buoyancy-assisted flow) is set for evaporation experiments. A similar by-pass loop was also installed on the secondary side in order to test UCHE thermal performance in parallel and counter flow configurations. Another UCHE is installed at the outlet of the test section in order to ensure full subcooled refrigerant when entering the pump. Finally, two thermal baths are used to control the inlet temperature of the glycol-water stream on the secondary side of the condenser and the reservoir temperature that sets the saturation pressure.

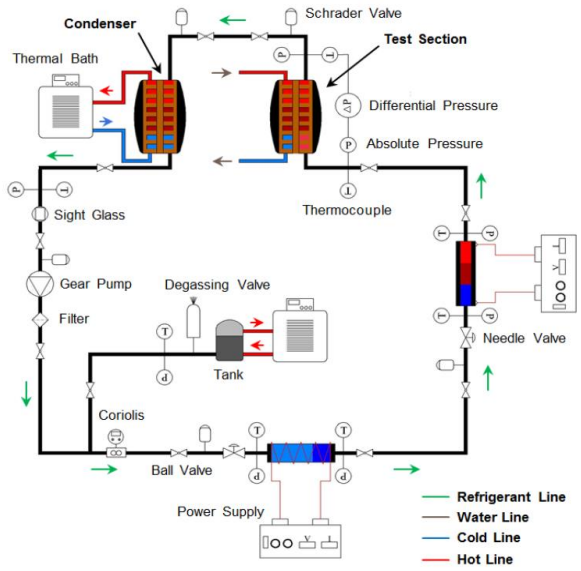

Figure 2 – Schematic of the LTCM's test facility showing the primary (refrigerant) side and its full instrumentation (T = temperature, P = absolute pressure and ΔP = pressure drop). Several ball valves and schrader valves are installed in the loop for charging/discharging the working fluid, vacuum and pressure tests. The secondary (water) side is not illustrated here, however its main components are: a Coriolis flow meter, an expansion tank, an air degassing valve and a thermal bath. The secondary side of the test facility also includes several temperature and pressure measurements and the loop is slightly pressurized (around 3 bar) to avoid trapping air during the formal experiments.

Figure 3 presents a picture of the primary side, mainly focused on the UCHE section that is partially insulated. A comprehensive overview on the UCHE characteristics, experimental apparatus, measurements and data reduction technique is reported in Amalfi et al. [10].

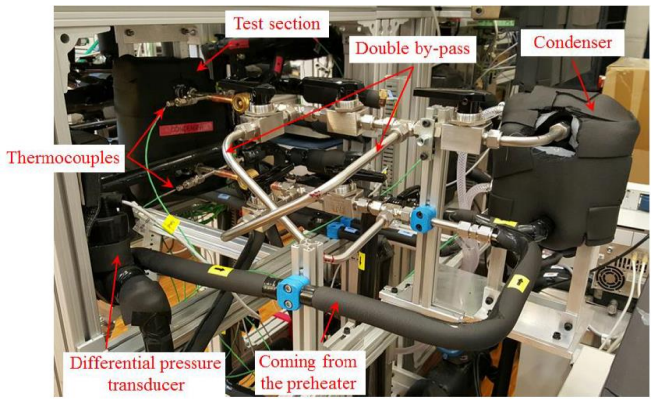

Figure 3 – Picture of the primary side of the test facility that includes details on the flow direction, temperature and pressure measurements and double by-pass. Note the presence of sight glasses at the inlet and outlet of the UCHE to have a visual access to the fluid flow.

On the other hand, Figure 4 depicts the flow schematic of the thermosyphon loop built at Nokia Bell Labs to characterize heat transfer performance of a passive two-phase system. The loop consists of a micro-scale evaporator, designed to cool 18 parallel heat sources (total power of 1.8 kW), that is connected via a riser and downcomer to the ultra-compact condenser (UCHE). The final application for the proposed thermosyphon is the cooling system of a Nokia's photonic service switch that operates with 18 line card and is a critical telecom equipment for optical transport and signal regeneration.

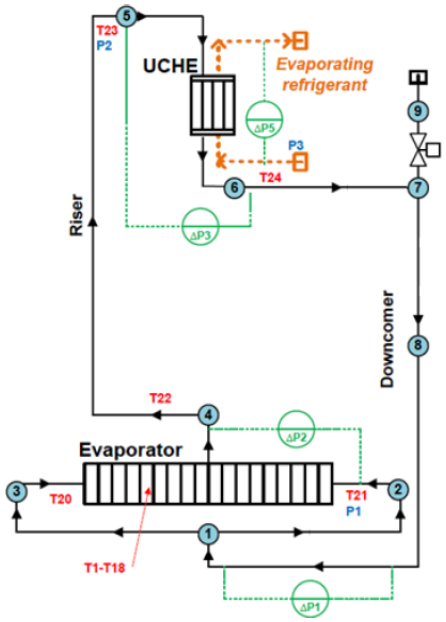

Figure 4 – Schematic of the Nokia Bell Labs' thermosyphon loop showing the location of temperature (red), absolute (blue) and differential pressure measurements (green). The point 9 in the loop is composed of a ball valve and a quick coupling for charging and discharging operation, as well as for vacuum and pressure tests.

With a reference to Figure 4, the refrigerant is subcooled at the inlet of the evaporator (points 2 and 3). The split-flow evaporator design helps to improve the flow distribution inside the inlet header and mitigate the pressure drops in order to achieve uniform cooling over the entire range of heat loads and filling ratios (FR is calculated as the initial liquid volume divided by the total internal volume of the thermosyphon). Then, the refrigerant is partially boiled at the outlet of the evaporator (point 4), and thanks to the buoyancy force, is passively driven upward to enter the condenser (point 5), where heat is rejected to a secondary side liquid-cooling loop, and the two-phase mixture is condensed back to liquid at the outlet of the UCHE (point 6). The gravity force then guides the liquid refrigerant downward (point 1) to enter the evaporator and start the cycle again. In this setup, the UCHE operates as a condensation-to-boiling counter-flow heat exchanger in which the heat removed from the 18 line cards is dissipated to a refrigerant pumped loop. R134a is the working fluid charged in both loops (pump-driven and gravity-driven thermosyphon).

Figure 5 shows a picture of the thermosyphon cooling system before completing the insulation. The UCHE and part of the riser and downcomer piping are visible. Steady-state experiments are performed under uniform and non-uniform heat load conditions.

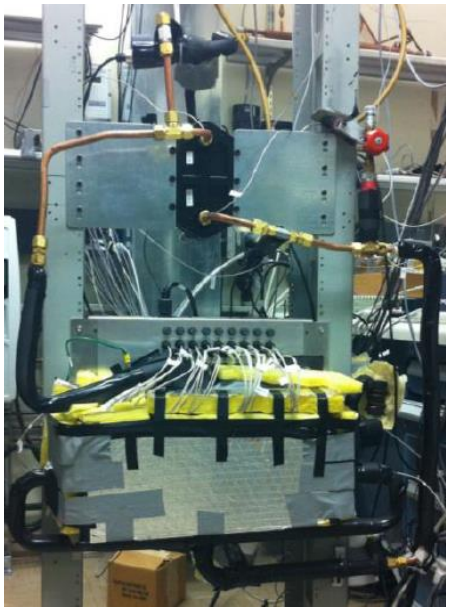

Figure 5 – Picture of the primary side (thermosyphon loop). The main components of the secondary side (pumped loop) are: a mass flow meter, two electrical preheaters, two control valves (upstream and downstream of the UCHE for flow and pressure control) and several K-type thermocouples, absolute and differential pressure transducers to measure fluid temperature, fluid pressure and pressure drops.

The reader can refer to Salamon et al. [11] and Amalfi et al. [12, 13] for additional details on the experimental apparatus, measurements and data reduction technique.

TEST SECTION (UCHE)

Figure 6 presents two pictures of the UCHE that has been designed by Prof. Thome and his team at LTCM and fabricated by Provides Metalmeccanica. The UCHE is composed of a double-side-copper finned plate, where the channel and fins geometry, as well as the headers are optimized to ensure high overall heat transfer coefficients, low pressure drops and uniform fluid distribution. These characteristics are appealing for its implementation in a gravity-driven thermosyphon loop where there is the need to minimize the pressure drops in order to achieve high thermal performance and high critical heat flux values (maximum heat removal of the system).

(a)

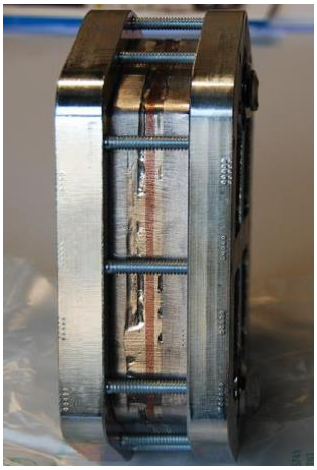

(b)

Figure 6 – Test section used in this study: (a) front view of the UCHE with visible inlet and outlet ports before connecting the piping. Similar fluid ports are machined on the secondary side (not shown here). The port-to-port length on both sides is 140 mm; (b) side view of the UCHE highlighting the stainless steel supporting frame.

The external dimensions of the UCHE are: H = 186 mm, W = 110 mm and D = 45 mm. The total internal volume is 44 cm^3 and its footprint heat transfer area is only 10 x 10 cm^2. The enhancement in heat transfer performance compared to traditional heat exchangers is mainly due to the two-phase flow patterns in micro-channels, plus the effective heat transfer area (fins allow about 11-fold increase in surface area compared to the footprint area). In the current design, the UCHE has one channel path for the primary side (refrigerant) and one channel path for the secondary side (water) with a thermal design power on the order of few kilowatts. It has to be mentioned that the same UCHE geometry is used for the tests performed at both locations LTCM and Nokia Bell Labs, however for the latter installation the UCHE has been black painted at the end of the fabrication process.

As can be seen from Figure 6, the copper finned plate is enclosed in a stainless steel supporting frame (tested up to 100 bar with an anticipated operational range of 5 to 20 bars) in order to hold the refrigerant pressure and avoid deformation due to pressure difference between the primary and secondary side (the latter may occur when the UCHE is implemented in refrigeration cycles). The use of a stainless steel enclosure is not anticipated to impact the thermal performance as the majority of the heat exchange occurs across the double-side copper finned plate, which is interior to the frame.

UNCERTAINTY ANALYSIS

Tables 3 and 4 present the minimum and maximum errors for the results discussed in the next section with reference to the LTCM and Bell Labs test facilities. The approach proposed by Kline and McClintock [14] is used to perform the propagation of errors from the initial measurements to the final results. The accuracies of the measured parameters are calculated considering the fixed error (defined during the calibration process) and the random error. The latter is evaluated as the multiplication of the coverage factor (equal to 2 for 95% level of confidence) and the measured standard deviation.

Regarding the results listed in Table 1 (LTCM's test facility): (i) the total pressure drop is directly measured from the inlet to the outlet of the primary side of the UCHE; (ii) the heat load is calculated by performing the energy balance across the secondary side of the UCHE in which water is always maintained in single-phase flow; (iii) the overall heat transfer coefficient is calculated from the heat load and the measured logarithmic mean temperature difference between the two fluids; (iv) the refrigerant side mass flow rate is measured thanks to a Coriolis flow meter. As mentioned previously, the reader is invited to consult Amalfi et al. [10] for more details.

Similarly for Table 2 (Nokia Bell Labs' test facility): (i) the heat load is measured at the evaporator section according to the electrical resistance and current flowing through the 18 parallel cartridge heaters; (ii) the overall heat transfer coefficient is calculated using the same technique as the one implemented in the LTCM's measurements; (iii) the thermosyphon mass flow rate is back calculated from the single-phase pressure drop and subcooling measurements taken at the inlet of the evaporator (Salamon et al. [11]); (iii) the subcooling at the outlet of the condenser (thermosyphon side) is evaluated by subtracting the fluid temperature from the saturation temperature. Additional information can be found in Amalfi et al. [13].

Table 1 – Uncertainty of the final results with reference to the LTCM's test facility.

MEASURED PARAMETER	VALUE
Total pressure drop	± 6.9 – 10.9%
Heat load	± 0.9 – 1.9%
Overall heat transfer coefficient	± 9.0 – 17.4%
Refrigerant mass flow rate	± 0.5% of the reading

Table 2 – Uncertainty of the final results with reference to the Nokia Bell Labs' test facility.

MEASURED PARAMETER	VALUE
Heat load	± 2.8%
Overall heat transfer coefficient	± 2.9 – 3.1%
Thermosyphon mass flow rate	± 3.4% of the reading
Subcooling	± 1.7 – 2.2%

EXPERIMENTAL RESULTS

Figures 7 and 8 show select key results obtained with the LTCM's test facility, while Figures 9, 10 and 11 are referred to the Nokia Bell Labs' apparatus. In particular, Figure 7 presents the effect of the working fluid on the total pressure gradient as a function of the refrigerant mass flow rate during adiabatic two-phase experiments.

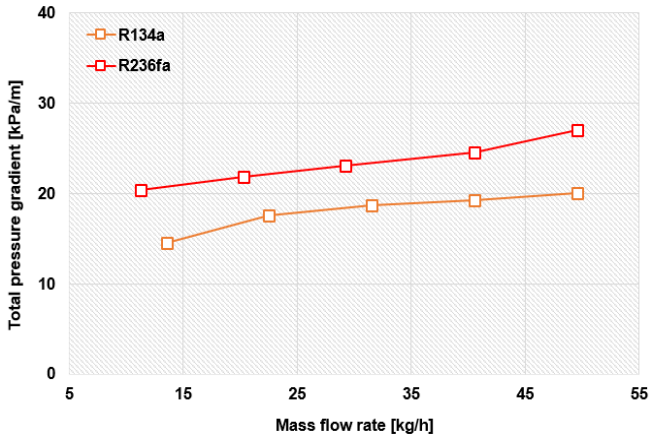

Figure 7 – Primary side total pressure drop as a function of the mass flow rate for two refrigerants (R134a and R236fa). Inlet saturation temperature is 30°C, local vapor quality is ≈ 0.02 and no heat is exchanged in the UCHE (adiabatic tests). These data are gathered envisioning the UCHE as the evaporator of a refrigeration cycle and this explain the low vapor quality (outlet condition from an expansion valve).

Two-phase flow is triggered upstream of the UCHE controlling the two electrical preheaters and there is no heat transfer taking place in the main test section. A differential pressure transducer is used to measure the total pressure drop from the inlet to the outlet of the UCHE. Consequently, the total pressure gradient takes into account the frictional, static and momentum pressure drop (over a reference length that is the UCHE port-to-port distance). It has to be mentioned that the momentum pressure drop is negligible here due to the small variation of vapor quality across the UCHE, which is only due to the change in pressure. As expected, the total pressure gradient increases with the refrigerant mass flow rate that is proportional to the square of the fluid velocity, while lower pressure drops are measured using R134a as the working fluid. In comparison with R236fa, R134a provides lower density and viscosity ratios (for a given saturation temperature), which are beneficial in reducing the shear stress between the liquid and vapor phases, and thus the total pressure drop. The highest value of pressure drop is 3.79 kPa for R236fa, while 2.81 kPa is measured for R134a.

Figure 8 shows a slightly increasing trend of the overall heat transfer coefficient with the heat load. During this set of experiments, the water and refrigerant mass flow rates on both sides are fixed, as well as the inlet vapor quality on the primary (refrigerant) side (about 0.5). Then, the heat load is increased by lowering the water inlet temperature (large LMTD).

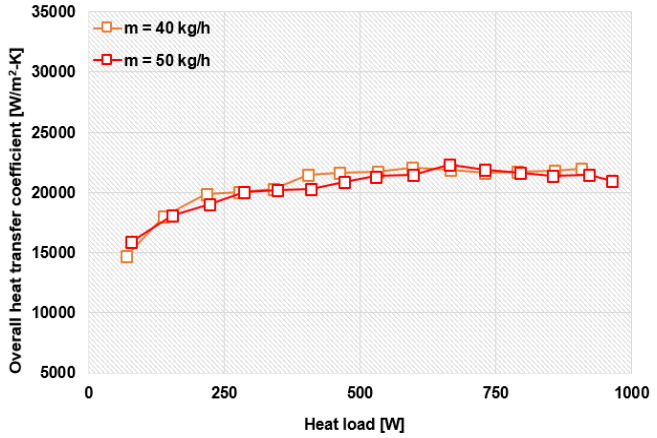

Figure 8 – Overall heat transfer coefficient as a function of the imposed heat load varying the primary side mass flow rate (40, 50 kg/h). Primary side is condensing flow using R236fa and the inlet saturation temperature is 31°C and vapor quality is ≈ 0.5. Secondary side is subcooled water with a mass flow rate of 60 kg/h and inlet temperature changing from 16 to 30 °C.

For condensing flow, the heat transfer coefficient decreases with the mean vapor quality and this can be justified by the fact that gravity-driven is the main two-phase heat transfer mechanism. According to the Nusselt theory [15], developed for laminar film condensation, the heat transfer coefficient is inversely proportional to the liquid film Reynolds number to the power 1/3. Consequently, the refrigerant side heat transfer coefficient has to increase with the heat load, being inversely linked to the mean vapor quality. On the other hand, the water side heat transfer coefficient is two times higher than the refrigerant side because of the larger thermal conductivity and mass flow rate. However, it decreases with the heat load due to a decrease in liquid thermal conductivity (the latter decreases with the mean temperature across the secondary side of the UCHE). The overall heat transfer coefficient is the result of two

competing trends, justifying the experimental data reported in Figure 8. Moreover, a small increase in refrigerant mass flow rate does not contribute in enhancing the UCHE thermal performance, when the condensing heat transfer process is mainly driven by gravity (film condensation). The lowest and highest overall heat transfer coefficients in condensing-to-single-phase flow are calculated to be about 15 and 22 kW/m^2-K, respectively.

As can be seen from Figure 9, the overall heat transfer coefficient measured in condensation-to-boiling experiments slightly increases with the heat load and R134a is the working fluid used on both sides of the UCHE. This is in agreement with the results presented in Figure 8. Furthermore, at low filling ratios, and in the region of low to medium heat loads, thermal performance is enhanced by the fact the two-phase mixture can reach the end of the UCHE without fully condensing. The minimum and maximum overall heat transfer coefficients from this set of experiments are 14 and 24 kW/m^2-K, respectively.

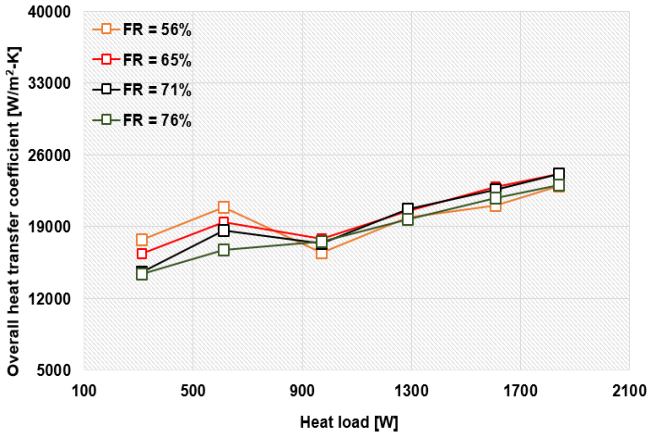

Figure 9 – Overall heat transfer coefficient as a function of the imposed heat load for several filling ratios. Secondary (boiling) side mass flow rate is 80 kg/h, inlet subcooling is ≈ 1 K and inlet pressure is 600 kPa.

Related to this aspect, Figure 10 shows the outlet subcooling on the primary side of the UCHE that increases with the heat load as more liquid is produced from the condensing flow. In addition, the outlet subcooling increases with the filling ratio, for a given heat load, due to the higher system pressure. The highest subcooling value is 1.1 K and referred to the highest filling ratio of 76% and maximum heat load of about 1840 W. It has to be mentioned that the thermosyphon loop operating with the UCHE provides excellent cooling capabilities as the variations of subcooling are minimized over the entire range of heat load. This is ideal for thermosyphon operation in order to minimize the evaporator thermal resistance (longer two-phase heat transfer length) and condenser thermal resistance (avoiding flooding).

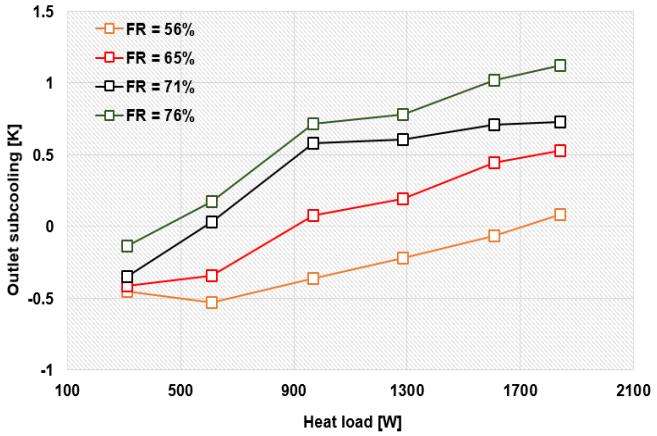

Figure 10 – Primary side outlet subcooling as a function of the imposed heat load for several filling ratios. Secondary (boiling) side mass flow rate is 80 kg/h, inlet subcooling is ≈ 1 K and inlet pressure is 600 kPa.

To conclude this section, Figure 11 reports the mass flow rate as a function of the heat load for different filling ratios (56-76%). As expected, the mass flow rate increases with the heat load because of the higher driving force in the thermosyphon, and also increases with the filling ratio, as more refrigerant is added to the system. Furthermore, the mass flow rate trends are not approaching to a plateau (or showing a decreasing trend), meaning that the thermosyphon is properly operating in the gravity-dominant regime [16]. Significant passive two-phase flow rate can be achieved in a well-designed thermosyphon loop, as the one built at Nokia Bell Labs, where the total height, from mid evaporator to mid condenser, is only 50 cm and the minimum and maximum refrigerant mass flow rates are 16.5 and 82 kg/h, respectively.

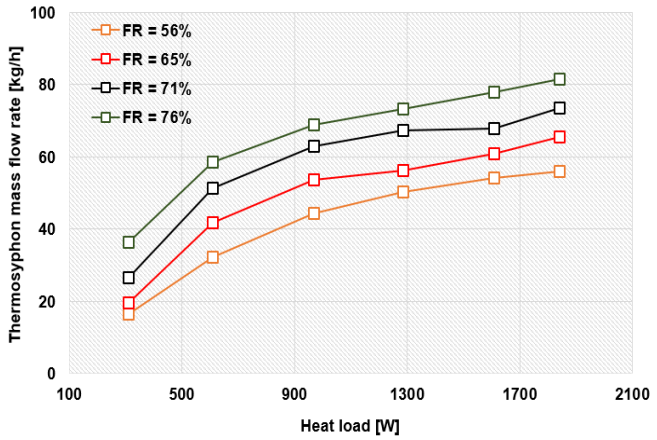

Figure 11 – Primary side mass flow rate as a function of the imposed heat load for several filling ratios. Secondary (boiling) side mass flow rate is 80 kg/h, inlet subcooling is ≈ 1 K and inlet pressure is 600 kPa. R134 is the working fluid used on both sides of the UCHE.

THERMAL PERFORMANCE ANALYSIS

As mentioned in introduction, edge datacenters represent a fast-growing market since they provide cloud computing and storage resources, while being closer to customers and thus reducing latency and improving performance. This section is focused on a thermal performance analysis to demonstrate that the cooling technology (presented in Figure 1) and thermal resistance circuit (depicted in Figure 12) is able to fulfill the requirements set in the following case study:

- 42-U rack architecture populated with 21 x 2-U servers for a total power dissipation of 20 kW/rack. In this case there is a sufficient height inside the servers to install gravity-driven thermosyphons;
- Servers are seen as entire heat sources with 2 CPUs per server to be cooled with a maximum allowable electronics temperature of 85ºC;
- Inlet temperature of the water on the secondary side of the overhead condenser (UCHE) is 30ºC and obtained by a dry-cooler;
- Main contributors to the total thermal resistance of proposed cooling technology are the TIM, server- and rack-levels thermosyphon.
- TIM is a permanent high-performance phase change material located between the heat source and evaporator base of the server-level thermosyphon;
- Rack-level thermosyphon thermal performance is based on the average height of 50 cm between mid-evaporator and mid-condenser (overhead heat exchanger), where the mass flow rate is assumed to be an average value over the number of thermosyphon loops;
- Overhead condenser is the UCHE presented in this study. The primary side is the condensing flow of the rack-level thermosyphon, while the secondary side is subcooled water circulated within a room-level pumped loop.

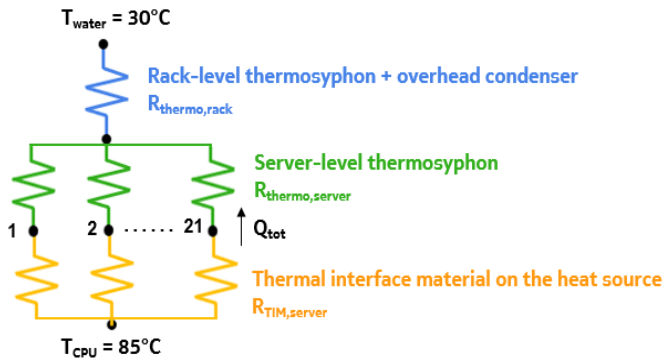

Figure 12 – Schematic of the thermal resistance circuit used for the thermal performance analysis in order to characterize the cooling capacity of the proposed passive two-phase system. Note that the server-level cooling loop is presented in terms of equivalent thermal resistances (TIM and thermosyphon) since the servers are composed of 2 CPUs.

It has to be pointed out that the phase change TIM is provided by Honeywell and the thermal resistance is calculated from the specified thermal impedance value. Server-level thermosyphon design and simulations are published in Amalfi et al. [8], while a schematic is reported in Figure 13. In addition, experimental results are included in Amalfi et al. [9, 17]. These references are used to extract the thermal resistance of 0.085 K/W. Reference measurements for the rack-level thermosyphon using the UCHE as a condenser are detailed in Amalfi et al. [13]. It has to be mentioned that the thermal resistance of the water-cooled overhead UCHE is extracted from the LTCM's measurements reported in Figure 8 and scaled based on the footprint area of the UCHE ($R_{th} \approx 0.004$ K/W).

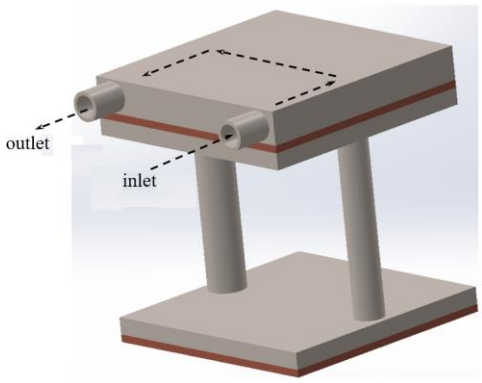

Figure 13 – Liquid-cooled thermosyphon designed for 2-U servers where the total height from the evaporator base and the top condenser lid is 7 cm. In the figure, the arrows indicate the flow direction of the secondary side that is the evaporator of the rack-level thermosyphon.

The total resistance for the cooling system can be expressed by the following formula:

$$\Delta T_{tot} = \left(T_{CPU} - T_{\text{water}}\right) = R_{\text{tot}} \times Q^{\text{CPU}}$$

where:

$$R_{tot} = \left(R_{\text{thermo}} + R_{TIM}\right)_{server} + \left(2 \times N_{\text{servers}} \times R_{\text{thermo}} \times \frac{1}{f}\right)_{rack}$$

$$= \left(0.085 + 0.0025\right) + 2 \times 21 \times 0.0058 \times \frac{1}{f}$$

thus:

$$\Delta T_{tot} = \left[\left(R_{\text{thermo}} + R_{TIM}\right)_{server} + \left(2 \times N_{\text{servers}} \times R_{\text{thermo}} \times \frac{1}{f}\right)_{rack}\right] \times Q^{\text{CPU}}$$

where f is an area enhancement factor that accounts for the need to scale the UCHE finned area to accommodate the increased heat dissipation for the nominally 20 kW rack.

Assuming an UCHE area enhancement factor of $f = 10$, this results in a total thermal resistance of 0.1119 K/W, which provides a total power dissipation of about 492 W/CPU (984 W/server) and 20.7 kW/rack (higher than 20 kW/rack as defined in the case study). Finally, we note that the majority (~78%) of the thermal resistance of the system is associated with the server-level thermosyphon loop and TIM, which requires that the rack-level UCHE finned area footprint be scaled significantly in order to achieve the desired 20 kW power dissipation level. This suggests that enhancements to the server-level thermosyphon loop can lead to significant increases in the overall power dissipation of the approach.

CONCLUSIONS

This paper continues the work presented at InterPACK 2019 and it is mainly focused on a new compact heat exchanger (UCHE), which can be implemented in the proposed passive two-phase cooling technology. The UCHE has been designed by Prof. Thome and his team at LTCM and manufactured by Provides Metalmeccanica S.r.l. (both companies are official partners of Nokia Bell Labs). The UCHE is composed of a double-side-copper finned plate enclosed in a stainless steel supporting frame to hold pressure during the formal two-phase tests. The UCHE's heat transfer performance is evaluated in a pumped loop, built at LTCM, and in a passive thermosyphon loop, built at Nokia Bell Labs. Results coming from both affiliations are in a good agreement with each other and they are discussed in terms of total pressure gradient, overall heat transfer coefficient, passive (thermosyphon) mass flow rate and condenser subcooling. The UCHE demonstrates excellent heat transfer performance, low pressure drops, requiring a very small form factor. These characteristics make the UCHE the ideal component for passive two-phase cooling systems. The present study also includes a thermal performance analysis for a small scale edge datacenter showing that the proposed cooling system is able to passively dissipate about 20 kW/rack with huge reduction in energy consumptions (low operating expenses) compared to conventional cooling systems deployed today. For this application, the overhead UCHE has to be redesigned with multiple plates and a slightly larger footprint area in order to accommodate higher heat dissipations compared to the baseline design.

ACKNOWLEDGEMENTS

The authors are delighted with the excellent collaboration among the three partners (Nokia Bell Labs USA, JJ Cooling Innovation Sàrl Switzerland and Provides Metalmeccanica S.r.l. Italy) for sharing design concepts, technical experiences and experimental results during the entire study.

REFERENCES

[1] R. Danilak, December 2017, Why energy is a big and rapidly growing problem for datacenters, Forbes Technology Council online journal.

[2] B. Whitehead, D. Andrews, A. Shah, G. Maidment, 2014, Assessing the environmental impact of datacenters part 1: background, energy use and metrics, Building and environment, vol. 82, pp. 151-159.

[3] J. Steman, May 2019, Datacenter.com signs EU code of conduct for energy efficiency in data centers as participant, Datacenter.com the foundation of digital economy.

[4] H. Rong, H. Zhang, S. Xiao, C. Li, C. Hu, 2016, Optimizing energy consumption for data centers, Renewable and sustainable energy reviews, vol. 58, pp. 674-691.

[5] W.M. Adams, November 2018, Power consumption in data centers is a global problem, The answer is global efficiency standards, Datacenter dynamics.

[6] L. Belkhir, A. Elmeligi, 2018, Assessing ICT global emissions footprint: trends to 2040 & recommendations, Journal of cleaner production, vol. 177, pp. 448-463.

[7] J.M. Lima, May 2019, Liquid cooling. A climate change weapon, Data economy magazine

[8] R.L. Amalfi, F. Cataldo, J.R. Thome, 2019, Design of passive two-phase thermosyphons for server cooling, Proceedings of the ASME International Technical Conference and Exhibition on Packaging and Integration of Electronic and Photonic Microsystems InterPACK-6386, USA.

[9] R.L. Amalfi, F. Cataldo, J.R. Thome, May 2020, The future of datacenter cooling: passive two-phase cooling, Electronics cooling magazine (as part of computer, datacenters, free air cooling, liquid cooling).

[10] R.L. Amalfi, N. Lamaison, J.B. Marcinichen, J.R. Thome, Flow Boiling and Condensation within an Ultra-Compact Microchannel Heat Exchanger, 2017, Encyclopedia of Two-Phase Heat Transfer and Flow IV, Volume 3: Micro-Two-Phase Cooling Systems, Editor: John Richard Thome, World Scientific Publishing Company, Singapore, pp. 1-67.

[11] T. Salmon, R.L. Amalfi, N. Lamaison, J.B. Marcinichen, J.R. Thome, 2017, Two-Phase Liquid Cooling System for Electronics, Part 1: Pump-Driven Loop, Intersociety Conference on Thermal and Thermomechanical Phenomena in Electronic Systems ITHERM, USA, pp. 667-677.

[12] R.L. Amalfi, T. Salamon, N. Lamaison, J.B. Marcinichen, J.R. Thome, 2017, Two-Phase Liquid Cooling System for Electronics, Part 2: Air-Cooled Condenser, Intersociety Conference on Thermal and Thermomechanical Phenomena in Electronic Systems ITHERM, USA, pp. 678-686.

[13] R.L. Amalfi, T. Salamon, N. Lamaison, J.B. Marcinichen, J.R. Thome, 2017, Two-Phase Liquid Cooling System for Electronics, Part 3: Ultra-Compact Liquid-Cooled Condenser, Intersociety Conference on Thermal and Thermomechanical Phenomena in Electronic Systems ITHERM, USA, pp. 687-695.

[14] S. Kline, F. McClintock, 1953, Describing uncertainties in single-sample experiments, ASME Mechanical Engineering, vol. 75, pp. 3-8.

[15] W. Nusselt, 1916, Die oberflächenkondensation des wasserdampfes, VDI-Zeitschrift, vol. 60, pp. 541-546 and 569-575.

[16] H. Bielinski, J. Mikielewicz, 2011, Natural circulation in single and two-phase thermosyphon loop with conventional tubes and minichannels, Heat transfer-mathematical modeling, numerical methods and information technology.

[17] R.L. Amalfi, F. Cataldo, J.B. Marcinichen, J.R. Thome, 2020, Experimental characterization of a server-level thermosyphon for high heat flux dissipations, Intersociety Conference on Thermal and Thermomechanical Phenomena in Electronic Systems ITHERM, USA (accepted for publication).